Journal of Thermal Analysis, Vol. 38 (1992) 2171-2179

THERMALLY ACTIVATED AND NON-ACTIVATED CHARGE TRANSPORT PROCESSES IN THE OXIDES Na_xMo_2

J. Molenda

INSTITUTE OF MATERIALS SCIENCE, ACADEMY OF MINING AND METALLURGY,
30–059 CRACOW, POLAND

The electrical properties of $Na_xM_{1+y}O_2$ (M = Mn, Co) were measured as a function of temperature under conditions of thermodynamic equilibrium for a quenched defect structure. The results of electrochemical studies of $Na_xM_{1+y}O_2$ are also presented. A correlation is demonstrated between the structures of the ionic and electronic defects in these materials and the potential changes of the cathode in $Na/Na^+/Na_xM_{1+y}O_2$.

Keywords: electrical properties, Na_xCoO_2, Na_xMnO_2

Introduction

Mechanistic studies of the intercalation processes in $A/A^+/A_xMX_2$ cells (A = alkaline metal, M = transition metal, X = O, S, Se) [1–6] have shown that the electronic structure of the cathode materials influences the character of the discharge curve. The amount of alkalimetal ions introduced electrochemically into the structure of MX_2 depends not only on the number of sites available for the ions (crystallographic voids), but also on the amount of states available for electrons in the electronic structure.

Electrons introduced in the electrochemical intercalation occupy the available states and cause the Fermi level to rise according to the state density function $N(E)$ of the cathode material. A high density of states near the Fermi level leads to a weak dependence of the potential on the alkali metal ion concentration and to a wide range for the variations in alkali metal ion concentration, whereas a low density of states near the Fermi level implies a strong compositional dependence of the potential and a narrow nonstoichiometry range in the alkali metal ion sublattice.

Relations between electronic and electrochemical properties have been noted earlier by other authors [7–9].

John Wiley & Sons, Limited, Chichester
Akadémiai Kiadó, Budapest

those compounds according to their electronic properties, it appears helpful to use a microscopic parameter such as the distance between neighbouring transition metal atoms. A comparison of the actual *M-M* distance ($R_{\text{M-M}}$) with the critical distance, R_c, given by Goodenough [10], permits prediction of the electronic properties of those compounds.

Classification of the compounds A_xMO_2 according to their electronic properties, based on the criterion of the *M-M* distance, is consistent with the classification according to their electrochemical properties. As shown previously [6], the compounds for which $R_{\text{M-M}} < R_c$ exhibit a discharge curve with a monotonous character and a wide nonstoichiometry range in the alkali metal ion sublattice, whereas those for which $R_{\text{M-M}} > R_c$ exhibit a discharge curve with a step-like character and a narrow nonstoichiometry range in this sublattice.

The present work demonstrates correlations between the electronic structure and the point defect structure and electrochemical properties of A_xMX_2, as illustrated by Na_xMnO_2 and Na_xCoO_2.

$Na_xM_{1+y}O_2$

The manganese bronze $Na_{0.7}MnO_2$ has a layered structure of P2 type, in which the MnO_6 octahedra are joined together along the edges, thereby forming $(MnO_2)_n$ layers. The Na^+ ions are located in the interlayer spaces. The results of thermogravimetric studies and of measurements of electrical conductivity and thermoelectric power at 600–1000 K at thermodynamic equilibrium and with quenched samples [2] indicate that this manganese bronze is a nonstoichiometric compound with the excess manganese atoms occupying sodium sites. The formation of defects can be described as follows:

$$2\,(\mathrm{Mn}^{\bullet}_{\mathrm{Mn}}\,\mathrm{V}'_{\mathrm{Na}})^{x} + 2\,\mathrm{O}_{\mathrm{O}} \rightleftharpoons \mathrm{Mn}^{\bullet\bullet\bullet}_{\mathrm{Na}} + \mathrm{O}_2 + \mathrm{Mn}^{x}_{\mathrm{Mn}} + 3\,e^- \qquad (1)$$

The negative sign of the thermoelectric power in a wide temperature range (300–1000 K) supports the conclusion that the deviation from stoichiometry introduces donor centers which are manganese ions at sodium sites (Eq. 1, Fig. 1).

Figure 2 presents the temperature dependence of the electrical conductivity for $Na_{0.7}Mn_{1+y}O_2$ samples with a quenched ionic defect structure for $y_1 = 0.11$ and $y_2 = 0.03$. It follows from Fig. 2 that the electrical conductivity has an activated character and the activation energy is 0.15 eV at 300–400 K, 1.0 eV at 400–460 K and 0.4 eV at 460–600 K.

Analysis of the electrical properties of manganese bronze at low temperatures indicates that this compound has the features of a partially compensated semiconductor. Figure 3 shows a qualitative scheme of its electronic structure. The deviation from stoichiometry in the manganese sublattice introduces deep donor levels. The ionization energy of the donor centers is of the order of 1 eV. At room temperature (i.e. at the

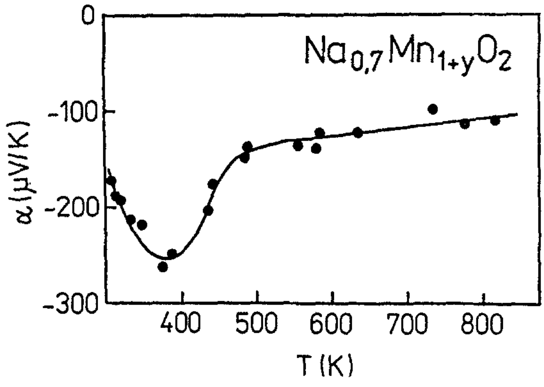

Fig. 1 Temperature dependence of thermoelectric power of manganese bronze

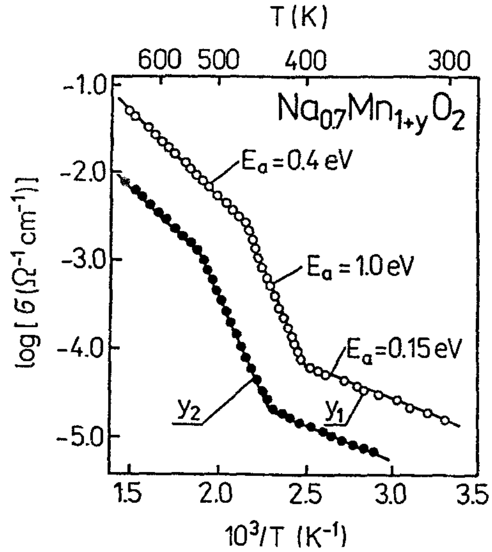

Fig. 2 Temperature dependence of electrical conductivity of $Na_{0.7}Mn_{1+y}O_2$ on the samples with the quenched ionic defect structure having composition: $y_1 = 0.11$, $y_2 = 0.03$

stoichiometry in the manganese sublattice introduces deep donor levels. The ionization energy of the donor centers is of the order of 1 eV. At room temperature (i.e. at the working temperature of a battery $Na/Na^+/Na_xMn_{1+y}O_2$, charge transport occurs in a narrow donor band partially ionized due to the presence of the acceptors (impurities) in the material. The activation energy of electrical conductivity in the lowest temperature range studied, 0.15 eV, corresponds to the activation energy of electron motion in a narrow donor band. The occurrence of localized electronic states in the manganese bronze is consistent with the condition $R_{Mn-Mn} > R_c$. The actual M—Mn distance in this material is 2.87 Å, whereas the critical distance R_c is 2.73 Å. At room temperature, the Fermi level is situated on the narrow donor band. The low density of the states near the Fermi level and their localization allows the introduction of a small concentration of electrons in the intercalation process (together with sodium ions). Figure 4 shows the OCV discharge curves for the bronzes $Na_{0.7}Mn_{1+y}O_2$ with $y_1 = 0.11$ and $y_2 = 0.03$. For the bronze with composition y_1, it is possible to introduce 0.04 moles of electrons. Further addition of electrons by intercalation brings about a jump of the Fermi level up to the middle of the E_D–E_C distance (0.5 eV), which corresponds to the potential jump in the discharge curve (Fig. 4). For the manganese bronze with $y_2 = 0.03$, which in comparison with y_1 has a lower concentration of donor centers (Mn_{Na}) the greater number of available states permits the introduction of a higher concentration of electrons (0.10 moles) in the intercalation process.

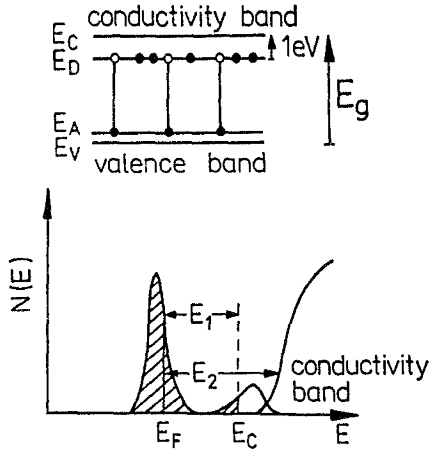

Fig. 3 Scheme of the electronic structure of manganese bronze

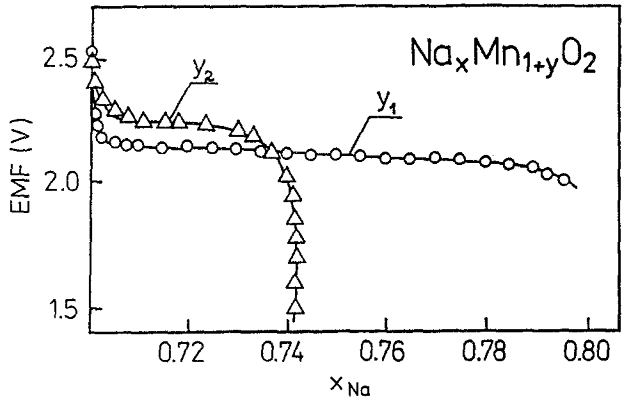

Fig. 4 Discharge curve (OCV) for manganese bronze $Na_{0.7}Mn_{1+y}O_2$; $1 - y_1 = 0.11$, $2 - y_2 = 0.03$

$Na_xCo_{1+y}O_2$

The cobalt bronze Na_xCoO_2, which has a P2 structure [1], is an example of a compound which, in the intercalation process at 300 K, undergoes a metal–non-metal transition.

In the stoichiometric cobalt bronze Na_xCoO_2, the Co^{3+} ions are present in the low-spin electron configuration t_{2g}^6. This state corresponds to a completely filled band, implying semiconducting properties of the compound. Nonstoichiometry in the sodium sublattice (V'_{Na}) leads to the occurrence of Co^{4+} ions. The low-spin configuration of Co^{3+} ($3d^6$) and Co^{4+}($3d^5$) ions corresponds to a situation where the t_{2g} band is not completely filled (electron holes), which should lead to metallic behaviour.

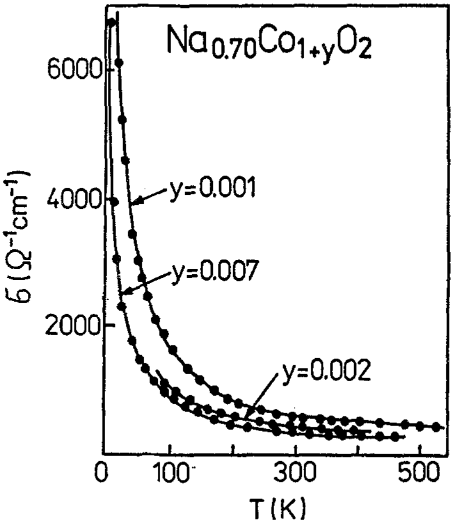

Fig. 5 Temperature dependence of electrical conductivity for $Na_{0.7}Co_{1+y}O_2$ of different y

Thermogravimetric studies and electrical conductivity and thermoelectric power measurements on the cobalt bronzes Na_xCoO_2 ($0.65 < x < 0.75$) at temperatures ranging from 600 to 1000 K under conditions of thermodynamic equilibrium, presented in detail earlier [11], have shown that this compound also exhibits deviation from stoichiometry in the cobalt-oxygen sublattice, associated with cobalt interstitials formed as donor centers in the following reaction:

$$Co_{Co}^{x} + 2\,V'_{Na} + 2\,O_O^{x} \rightleftarrows Co_{Na}^{\bullet\bullet} + O_2 + 4\,e^- \qquad (2)$$

Electrons from the ionization of donor centers recombine with electron holes associated with nonstoichiometry in the sodium sublattice and thereby lower their effective concentration:

$$Co^{x}_{Co} + 2\,O^{x}_{O} + 2\,V'_{Na} + 4h^{\bullet} \rightleftharpoons Co^{\bullet\bullet}_{Na} + O_2 \qquad (3)$$

Charge transport takes place in the t_{2g} band, the width of which ensures the metallic properties of the cobalt bronze [1].

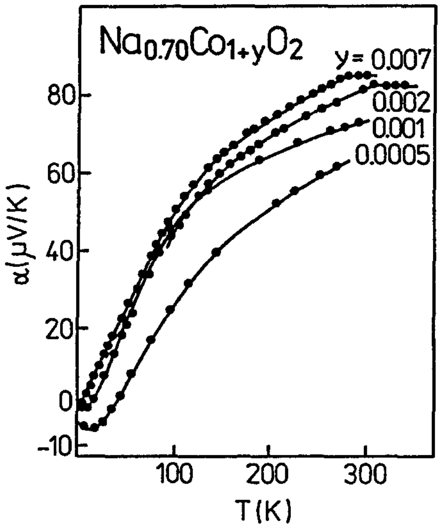

Fig. 6 Temperature dependence of thermoelectric power for $Na_{0.7}Co_{1+y}O_2$ of different y

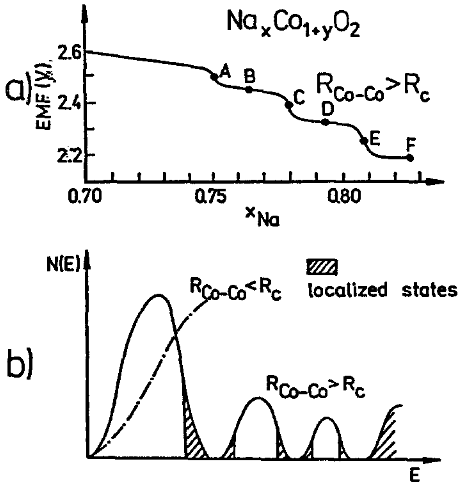

Fig. 7 a) Discharge curve (OCV) for cobalt bronze $Na_{0.7}CoO_2$.
Points A, B, C, D, E and F denote the composition x_{Na} where the work of the cell was broken up. b) Density of states of $Na_xCo_{1+y}O_2$

Figures 5 and 6 present as examples the low-temperature dependence of the electrical conductivity and thermoelectric power for the cobalt bronzes. $Na_{0.7}Co_{1+y}O_2$ at different values of y. The character observed for these relations confirms the metallic properties, although the values of the thermoelectric power, of the order of 100 μV/deg, indicate that this is not classical metallic behaviour.

Measurements of the lattice parameters of the cobalt bronzes $Na_xCo_{1+y}O_2$ obtained in a high-temperature solid-state reaction, with x ranging from 0.65 to 0.75, indicate that the parameter a (the Co-Co distance) is practically constant and does not exceed a criti-

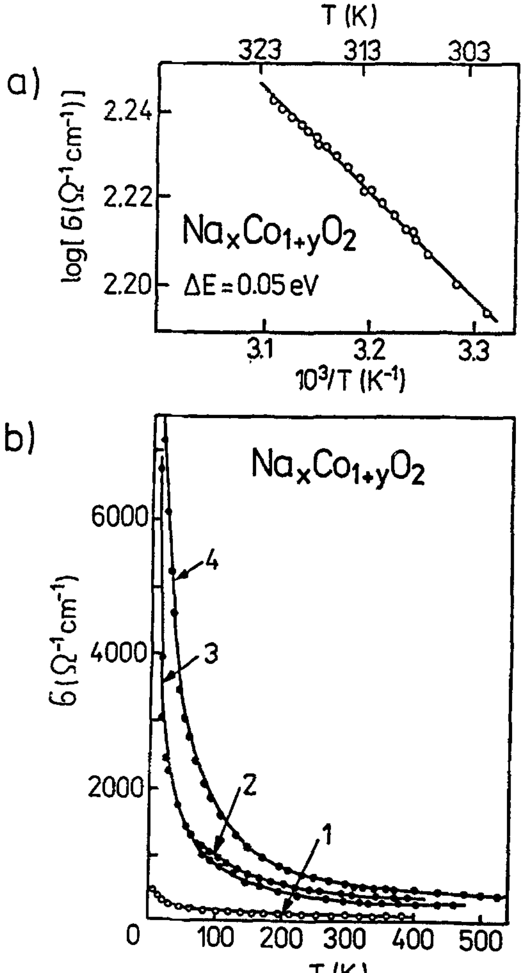

Fig. 8 Temperature dependence of electrical conductivity of intercalated $Na_xCo_{1+y}O_2$ a) for the composition x_{Na} = C (Fig. 7), b) curve 1 – for the composition x_{Na} = D (Fig. 7) curves 2, 3, 4 – starting material with different y

cal value of 2.822 Å. This is consistent with the observed metallic behaviour of the cobalt bronzes obtained at high temperatures. In electrochemical intercalation (T = 300 K), the parameter a changes from 2.815 to 2.845 Å as x_{Na} changes from 0.70 to 0.85. Under these conditions, the Co-Co distance reaches the critical value, R_c, which implies splitting of the effective energy band. The modification of the electronic structure of the cobalt bronzes toward the formation of a narrow-band structure is reflected in the step-like character of the discharge curve (Fig. 7). In order to demonstrate that the potential jumps in the discharge curve (Fig. 7) are associated with the Fermi level variations resulting from the filling of consecutive bands in a narrow-band structure of intercalated cobalt bronze, the electrical properties of the cathode material were measured at some characteristic points of the discharge curve (i.e. in the range of the potential jump and on the plateau). As an example, Fig. 8a presents the temperature dependence of the electrical conductivity for a cobalt bronze removed from a working cell at point C on the discharge curve (Fig. 7). The activation energy of the electrical conductivity corresponds to the magnitude of the potential jump in the discharge curve, i.e. 0.1 eV. It should be emphasized that the starting material, $Na_xCo_{1+y}O_2$ ($0.65 < x < 0.75$), exhibits metallic behaviour in the whole range of its stability (4–1000 K) [1].

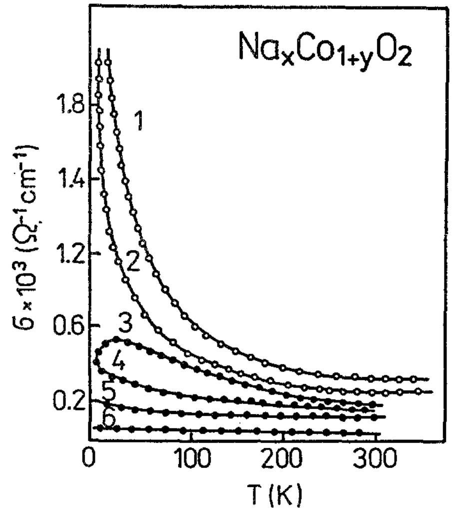

Fig. 9 Temperature dependence of electrical conductivity of cobalt bronzes. o – for the starting material:
(1) – $Na_{0.7}Co_{1.01}O_2$, (2) $Na_{0.75}Co_{1.01}O_2$
• – for their intercalated material:
(3) – $Na_{0.75}Co_{1.01}O_2$, (4) – $Na_{0.77}Co_{1.01}O_2$, (5) – $Na_{0.79}Co_{1.01}O_2$, (6) – $Na_{0.8}Co_{1.01}O_2$

Further intercalation, up to the composition denoted by point D on the discharge curve (Fig. 7), leads to the cobalt bronze regaining metallic properties (Fig. 8b), but these are different from those of the starting material. The activated character of the electrical conductivity for the cathode material with composition corresponding to the potential jump in the discharge curve (points A, C and E, Fig. 7), with the activation energy corresponding to the magnitude of the potential jump, and metallic properties (but different from those of the starting material) for the composition in the middle of the potential plateau (points B and D, Fig. 7), are direct evidence of the existence of partial bands which appear in cobalt bronze in the electrochemical intercalation. Figure 9 shows the changes in electrical properties as a function of the intercalation degree (increasing R_{Co-Co}) in the lowest temperature range. A comparison of the properties of the starting bronze with those after gradual intercalation indicate the occurrence of Anderson localization [1].

* * *

The author is grateful to Prof. S. Mrowec and Dr. A. Stoklosa for helpful discussions.

References

1 J. Molenda, Phys. Stat. Sol. (b), 122 (1984) 591.
2 J. Molenda, A. Stoklosa and Do Than, Solid State Ionics, 24 (1987) 33.
3 J. Molenda and A. Stoklosa, Solid State Ionics, 38 (1990) 1.
4 J. MOlenda and A. Stoklosa, Solid State Ionics, 36 (1989) 43.
5 J. Molenda, A. Stoklosa and T. Bak, Solid State Ionics, 36 (1989) 53.
6 J. Molenda, Phys. Stat. Sol (b), 165 (1991) 419.
7 D. M. Schleich and M. Rosso, Solid State Ionics, 5 (1981) 383.
8 M. Balkanski, K. Kambas, C. Julien and J. Hammerberg, Solid State Ionics, 5 (1981) 387.
9 M. Voinov, Proc. Lithium Battery Symp., Electrochem. Soc. Fall Meeting, 1980.
10 J. B. Goodenough, Progress in Solid State Chemistry, Ed. H. Reiss, Vol. 5, Pergamon Press, Oxford 1971, p. 279.
11 A. Stoklosa, J. Molenda and Do Than, Solid State Ionics, 15 (1985) 211.

Zusammenfassung — Unter den Bedingungen eines thermodynamischen Gleichgewichtes wurden die elektrischen Eigenschaften von $Na_xM_{1+y}O_2$ (mit M= Mn, Co) als Funktion der Temperatur bestimmt. Zusätzlich wurden die Ergebnisse der elektrochemischen Untersuchungen von $Na_xM_{1+y}O_2$ dargelegt. Es wird eine Korrelation zwischen der Struktur von Ionen- und Elektronendefekten dieser Substanzen und der Potentialänderung an der Kathode in einer $Na/Na^+/Na_xM_{1+y}O_2$ Zelle gezeigt.